ISSN: 1410-8917
Jurnal Kimia Sains & Aplikasi
e-ISSN: 2597-9914

Jurnal Kimia Sains dan Aplikasi 21 (4) (2018): 205–210

Jurnal Kimia Sains dan Aplikasi
Journal of Scientific and Applied Chemistry

Journal homepage: http://ejournal.undip.ac.id/index.php/ksa

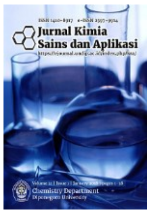

Lowered Sintering Temperature on Synthesis of $La_{9.33}Si_6O_{26}$ (LSO) – $La_{0.8}Sr_{0.2}Ga_{0.8}Mg_{0.2}O_{2.55}$ (LSGM) Electrolyte Composite and the Electrical Performance on $La_{0.7}Ca_{0.3}MnO_3$ (LCM) Cathode

Yoga Trianzar Malik [a], Atiek Rostika Noviyanti [a,*], Dani Gustaman Syarif [b]

[a] Physical-Inorganic Chemistry Laboratory, Department of Chemistry, Faculty of Mathematics and Science, Universitas Padjadjaran
[b] Technophysics Laboratory, Applied Nuclear and Science Centre, Badan Tenaga Nuklir Nasional (PSTNT-BATAN)

* Corresponding author: atiek.noviyanti@unpad.ac.id

https://doi.org/10.14710/jksa.21.4.205-210

Article Info

Article history:
Received: 15 August 2018
Revised: 20 October 2018
Accepted: 22 October 2018
Online: 31 October 2018

Keywords:
SOFC, LSO-LSGM, ASR, LCM/LSO-LSGM/LCM

Abstract

Solid oxide fuel cell (SOFC) is the device that can convert chemical energy into electricity with highest efficiency among other fuel cell. $La_{9.33}Si_6O_{26}$ (LSO) is the potential electrolyte at intermediate operation temperature SOFC. Low ionic conductivity of lanthanum silicate-based electrolyte will lead into bad electrical performance on lanthanum manganite-based anode. In this study, LSO was combine with $La_{0.8}Sr_{0.2}Ga_{0.8}Mg_{0.2}O_{2.55}$ (LSGM) electrolyte by using conventional solid state reaction to enhance the electrical performance of LSO on LCM cathode. However, pre-requisite high sintering temperature on preparation of LSO-LSGM composite will lead into phase transition phase of LSGM that may affect in decreasing the electrical performance. This study resulted that lowered sintering temperature from its ideal temperature still give an improved electrical performance of LCM/LSO-LSGM/LCM symmetrical cell. The ASR value is 0.14 $\Omega.cm^2$ which much lower than its analogous symmetrical cell, LSM/LSO/LSM that was reported before.

1. Introduction

In the recent years, electricity consumption is noted a tremendous value as 20,201.301 TWh all over the world. Besides, the emission of carbon dioxide had reached 32,294 Mt in 2015 by fuel usage [1]. This issue has led an attraction of evolutionary electrical generator that reflects an eco-friendly fueled device in which converting chemical energy into electricity such as solid oxide fuel cell (SOFC). SOFC can generate the electricity up to 10MW [2] which has the highest efficiency 40-60% among any other fuel cells [3]. SOFC itself consists of electrolyte and electrode components which was fabricated from many rare-earth elements. In order to obtain a good electrical output, SOFC must have been operated at high temperature. However, much higher temperature will lead the cell into incompatibility in physicochemi-mechanical properties that drives the cell toward electrical deficiency and even destruction due to chemical instability of components based on high-temperature reaction occurred.

Lanthanum silicate apatite (LSO) is a potential electrolyte at low temperature. On the other hand, lanthanum gallate (LGO)-based electrolytes are known as good electrical performance electrolytes at intermediate temperature. LSO had been combined with other electrolyte material such as yttrium stabilized-zirconia (YSZ) and samarium doped ceria (SDC). But this combination still showed no significant effect in conductivity. LSO-YSZ showed a low conductivity 1.72 x 10^{-4} Scm^{-1} at 973K [4]. LSO-SDC also showed low conductivity at 9.27×10^{-3} S/cm^{-1} at 1073K [5]. Low conductivity might affect the electrical performance. $La_{9.33}Si_6O_{26}$ (LSO) relatively has low ionic conductivity as 0.002 $S.cm^{-1}$ at 1073K [6] in comparing with $La_{0.8}Sr_{0.2}Ga_{0.8}Mg_{0.2}O_3$ (LSGM) electrolyte which has a good conductivity value as 0.166 $S.cm^{-1}$ (1073K) [7]. The combination of those electrolytes was expected to obtain a good electrical performances of its bulk material and the interaction with lanthanum manganite ($LaMnO_3$)-based cathode such as a $La_{0.7}Ca_{0.3}MnO_3$ (LCM). LCM itself has a magnificent electrical conductivity as ~200 $S.cm^{-1}$ at 1173K [8]. Both lanthanum silicate apatite and lanthanum gallate-based electrolytes were known having good chemical stability with $LaMnO_3$ cathode [9, 10].

On the other hand, Shi *et.al.* [5] reported high temperature sintering on the preparation of LSO-SDC electrolyte composite as 1823K. While Noviyanti *et.al.* [4] also showed high sintering temperature on LSO-YSZ electrolyte as 1673K. LSO is melting at above 2273K based on its phase diagram [11], while LSGM starts to melt at ~1773K [12]. In order to fabricate a good combination of LSO-LSGM, the solid state reaction must take place above 1673K based on Tamman's rules for ideal sintering temperature [13]. However, this temperature will lead the phase conversion of LSGM at high temperature [14] which lead a tendency of the lowering electrical performances of individual components. Hence, lowering the sintering temperature below 1673K was designated to decrease the effect of this phase transition. This research aimed to synthesize the electrolyte composite of LSO-LSGM at below its Tamman's temperature and study the electrical performance of LSO-LSGM electrolyte composite on LCM cathode.

2. Experimental

2.1. LSO synthesis

LSO was firstly synthesized from La_2O_3 (Aldrich, 99.999%, *trace metal*), $Na_2SiO_3.5H_2O$ (Aldrich, 95%), and NaOH (Merck, 98%) via hydrothermal method suing 100 mL autoclave [15] by modification of synthesis time (7 days synthesis at 313K) based on Noviyanti *et.al.* [16].

2.2. LSO-LSGM composite preparation

LSGM electrolyte was obtained from Sigma-Aldrich (99.999%, *trace metal*). Both materials with ratio 51:49 (LSO-LSGM) were mixed by using mechanical milling using zirconium ball for 24h. Then it was sintered at 1273K for 36h using gradual steps sintering temperatures as 573K, 1073K, and 1273K by milling at each step.

2.3. Characterization of LSO-LSGM composite and LCM/LSO-LSGM/LCM performance analysis

The result was recorded using Rigaku SmartLab X-Ray Diffraction with Cu-Kα radiation, λ= 0.15418nm, T=298K, v=0.02° min^{-1}. The actual composition was studied using SEM-EDS analysis (Hitachi-EDAX Team). This mixed material then was uni-axially pressed into a pellet (area=1,76cm^2, and thickness = 0.15cm). LCM cathode was synthesized from La_2O_3 (Aldrich, 99.999%, *trace metal*), $CaCO_3$ (Merck, 99.9%), and MnO_2 (Merck, 99.9%) using conventional solid state reaction [17]. The electrolyte pellet was re-sintered at 1523K for densification. It was furthermore coated with LCM cathode slurry at both side by cellulose acetate in DMF as a binder. The sintering process was prerequisite to eliminate the binder at 1123K for 1h. The prototype of symmetrical cell LCM/LSO-LSGM/LCM that was attained from this process then was tested for electrical performance using EIS method at ambient air atmosphere by using LCR Meter GW Instek 8105G in frequency range of 20Hz – 5MHz. In order to get ASR value, the resistance that was obtained from EIS measurement and fitted with ZView® then calculated.

3. Results and Discussion

3.1. Preparation of LSO-LSGM electrolyte composite

LSO as the precursor was successfully synthesized using hydrothermal method and then the structure was analyzed using XRD. The XRD pattern (Fig. 1) showed a good refinement of the LSO phase within 7 days synthesis time. The data analysis was using *Highscoreplus*©. The XRD pattern as shown in Fig. 1 was pointing a characteristic peak at 2θ = 30.84° (2 1 1) and 2θ = 31,07° (1 1 2) with the relative intensity as 100% and 71% respectively. All the peak was matched with the standard ICSD No.98-015-5624 with Gof (Goodness of fit) as 2.1522. The impurities phase as La_2SiO_5 that was found in [16] and another phase like $La_2Si_2O_7$ in Sakao *et.al.* [6] were not found in the LSO pattern. This phenomena justified the formation of LSO crystallite phase. LSO itself has p63/m space group (*a*=*b*=9,7271(8) *c*=7,1863(6)) that was accorded to LSO synthesized by Noviyanti *et.al.* [16] with cell unit volume as 588.87Å^3.

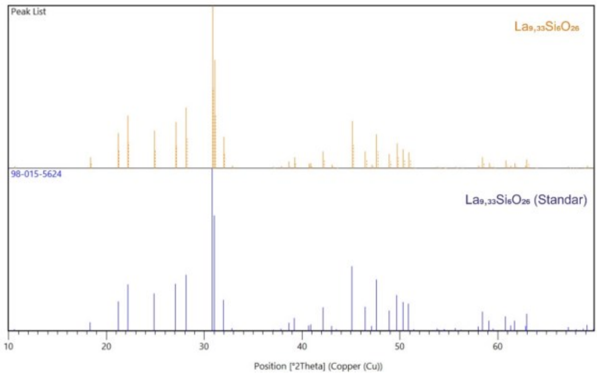

Fig. 1. XRD pattern of $La_{9,33}Si_6O_{26}$ (LSO)

LSO-LSGM electrolyte composite was successfully synthesized using conventional solid state method at 1473K. Fig. 2 depicted distinguishable peak from each component phase of LSO and LSGM respectively while the inset represented an actual XRD pattern. The diffraction peaks do not show another peak impurity that might emerge from both materials. The diffraction denotes two main peak in which correlating with LSO at 2θ = 30.3396 (2 1 1) and with LSGM at 2θ = 32.1447 (0 1 1). The crystallinity from both peaks can be determined through a ratio calculation of peak height (h) per total peak intensity (I) [18] as shown in Fig. 3. The percentage of crystallinity for both peaks were calculated as 65.86% and 70.70%. This value confirmed the good crystallinity for electrolyte composition (51:49) which was obtained at lowered sintering temperature.

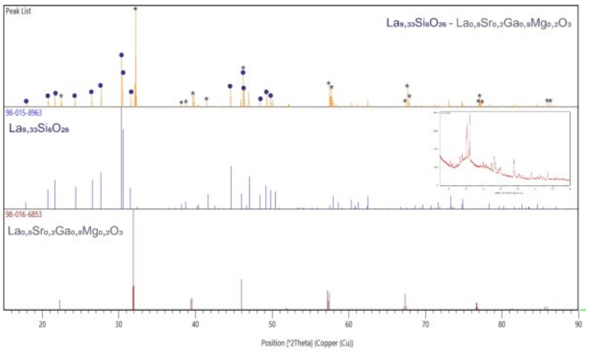

Fig. 2. XRD peaks of LSO-LSGM and the inset pointed the bare data of LSO-LSGM XRD pattern

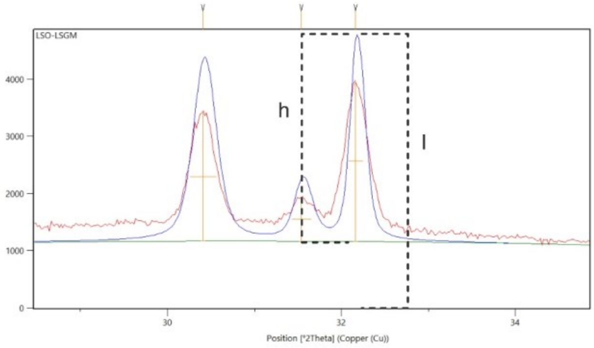

Fig. 3. Peak diagram for crystallinity percentage ratio calculation. This figure showed the peak height (h) and the peak total intensity (I) of LSO-LSGM peak at around 2θ = 32°. This figure is also denoting the peak data for crystallinity percentage calculation as explained before.

The LSO peak shifted toward lower degree rather than its ICSD standard from 2θ = 30.71 to 30.34 which indicated unit cell volume expansion (Table 1.) while the LSGM peak shifted toward higher degree from 2θ = 31.80 to 32.14 that was indicating shrinkage of unit cell volume as shown in Table 1. The shifting was depicted in a zoomed diffraction peak as shown in Fig. 4. The shrinkage of LSGM peak was estimated from phase transition from orthorhombic to cubic that was occurred at 1073K [5]. In this study, LSGM phase was found in cubic crystal structure with P m -3 m space group in accordance with Philippeau *et.al.* [19] and Rahmawati *et.al.* [20] study. $La_{1-x}Sr_xGa_{1-y}Mg_yO_{3-\delta}$ has orthorhombic-based crystal structure and gradually change to primitive cubic structure as increasing Sr and Mg dopping to La and Ga [21].

Table 1. LSO and LSGM lattice parameter

Phase	a/ Å	b/ Å	c/ Å	V (Å³) theoretical	V (Å³) practical	Annotation
LSO This study	9.722(8)	9.722(8)	7.237(9)	587.92	592.57	Expansion from standard
LSO [16]	9.722(1)	9.722(1)	7.186(1)	-	588.219	
LSGM	3.896(7)	3.896(7)	3.896(7)	60.01	59.17	densification from standard
LSGM [19]	3.919(4)	3.919(4)	3.919(4)	-	60.19	

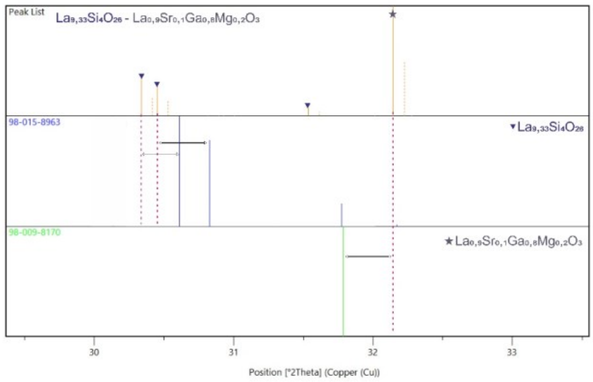

Figure 4. The zoomed 2θ degree that showed the shifting of LSO and LSGM peak before its individual standard

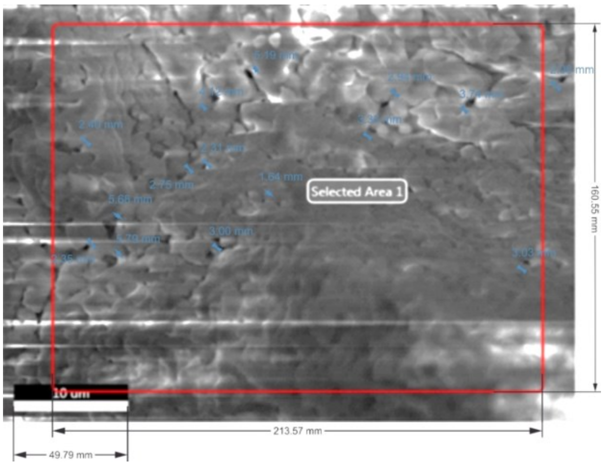

Fig. 5 Selected area of EDS analysis on LSO-LSGM electrolyte composite

SEM-EDS analysis at cross-sectional LSO-LSGM electrolyte pellet was carried out to study the actual composition of LSO-LSGM in the composite. Fig. 5 showed relatively a dense LSO-LSGM electrolyte with low porosity. The porous that was formed reflects a small diameter as 0.67±0.25µm at 15 points based on the length calculation technique by using parallel dimension tool in CorelDraw ©2018. This porous might refer as discontinued macroporous which lead to a relatively dense electrolyte.

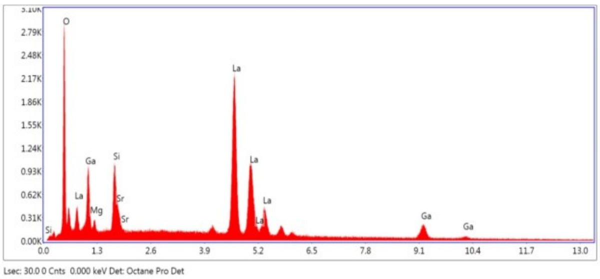

Fig. 6. EDS Spectrum of LSO-LSGM electrolyte composite

The expected theoretical composition in this study was 0.5110g (LSO): 0.4927 (LSGM). This value then was calculated to each percentage of sample components in LSO-LSGM as shown in Table 2. The percentage signified an error between theoretical and practical value as average 0.19. This is confirming that LSO-LSGM composite was formed as expected in such composition. This value took no significant effect to the composition, as diffraction data showed no additional peak of impurity and EDS spectrum (Fig. 6) showed every single component in LSO-LSGM.

Table 2. Percentage of EDS composition in LSO-LSGM electrolyte composite

Element	Mass from EDS/ %	Theoretical mass/ %	Error
La	55.76	58.00	0.04
Si	5.47	4.58	0.16
O	22.04	21.19	0.04
Ga	10.05	11.58	0.15
Sr	4.29	3.64	0.16
Mg	2.39	1.01	0.58
Total	100	100	-

3.2. Electrical Performance of LCM/LSO-LSGM/LCM

Area specific resistance (ASR) is value of total resistans (Rtot = R_1, R_2, and R_3) with geometrical factor-dependent (A) at which being obtained from value fitting of Nyquist plot using ZView. The ASR value was calculated using an equation $ASR_{elektrode} = Rtot \cdot A/2$; $Rtot = R_1 + R_2 + R_3$ [22]. The Nyquist plot itself was obtained from EIS measurement. **Fig. 7** depicted Nyquist diagram for symmetrical cell LCM/LSO-LSGM/LCM. From the diagram, increasing in temperature led to shrinking in semi-circle which indicated the decreasing of total polarization resistance (Rtot = Rs+Rp) as expected. At lower frequency, Rp was pointed as a small 'tail' that may refer to the second semicircle as the existence of an electrode on the electrolyte [23]. That was confirmed that polarization resistance could occur at this symmetrical cell that was containing LCM cathode. Rp was pointed by R_1, R_2, and R_3 symbols as at its equivalent circuit in Fig.7 and noted in Table 3.

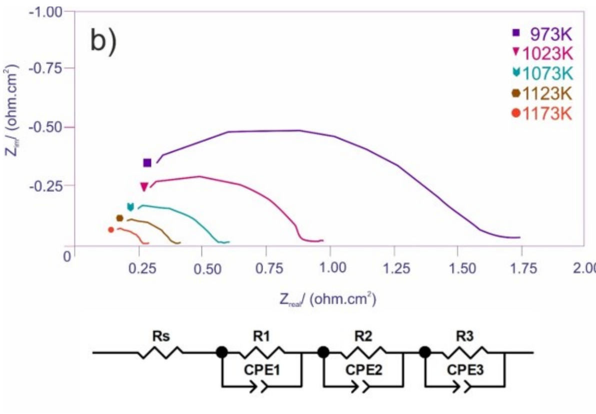

Fig. 7. Nyquist plot of symmetrical cell LCM/LSO-LSGM/LCM and its equivalent circuit

Ohmic resistance (Rs) refers to activity of ionic conductivity that was possessed by the bulk phase of electrolyte. The lower values indicated higher ionic activity on electrolyte. LSGM as the reinforcement in LSO-LSGM composite was estimated play a great role to lower the resistance rather than LSO. The conductivity of LSGM is 0.166 S.cm^{-1} (1073K) [7] which is much larger than LSO, 0.002 S.cm^{-1} at 1073K [6].

Table 3. ASR value of symmetrical cell LCM/LSO-LSGM/LCM at various temperature

T/ K	Rs/ Ω	R_1/ Ω	R_2/ Ω	R_3/ Ω	ASR/ Ω.cm^2
1.173	0.054929	0.045168	0.063698	0.052569	0.142697
1.123	0.104130	0.000174	0.013119	0.252582	0.235014
1.073	0.145430	0.000167	0.011866	0.380685	0.347135
1.023	0.141090	0.000166	0.023892	0.697891	0.638151
973	0.077042	0.419406	0.261264	0.624422	1.153608

ASR value denoted higher value than its ohmic resistances at all temperature as shown in Table 3. This behavior indicated the dominant ionic conduction activity of electrolyte bulk phase rather than electronic conductivity and electrochemical activity at cathode. The diffusion transfers resistance (R_3) gave a great contribution on ASR value. R_3 shows diffusion transfer of oxide ion (O^{2-}) at triple phase boundary at electrolyte/electrode interface. This might correlate with low reactivity of lanthanum silicate apatite and lanthanum gallate-based electrolyte with lanthanum manganite-based cathode [10]. However, the Mn diffusion on LSO electrolyte and Si diffusion on LCM electrode [9] had a probability to block reaction site on TPB at which lowering the electrochemical activity and increasing the value of ASR.

On the other side, Cao and Jiang [24] reported ASR value of analogous symmetrical cell with the cell in this study, LSM/LSO/LSM as 1.74 Ω.cm^2 (1173 K) which is 12.43 times larger than was found in this experiment. It can be rationalized that the electrical conductivity might take effect on this change. The conductivity of $La_{0.7}Ca_{0.3}MnO_3$ cathode was reported as 264 S.cm^{-1}at 1223 K [8] which much larger than conventional cathode, $La_{0.7}Sr_{0.3}MnO_3$ (200 S.cm^{-1} at 1273 K) [25]. This behavior could confirm that the lowered sintering temperature on LSO-LSGM electrolyte composite preparation might have been taken no significant effect on electrical performance and it was predicted that lowered sintering temperature could resist the phase transition of LSGM.

4. Conclusion

LSO-LSGM electrolyte composite was successfully synthesized using conventional solid state method. The lowered sintering temperature was expected to sustain a phase stability of LSGM as the reinforcement material at elevated temperature. The electrical performance of LSO-LSGM electrolyte composite on LCM cathode in LSM/LSO-LSGM/LCM showed a better value than its analogous symmetrical cell LSM/LSO/LSM. ASR value of LCM/LSO-LSGM/LCM denoted as 0.14 Ω.cm^2 at 1173K. The value showed that the lowered sintering temperature of LSO-LSGM composite formation still give an improved electrical performance of LSO-LSGM composite on LCM cathode.

5. Acknowledgement

This research was supported by Physics-Inorganics Chemistry Laboratory and PSTNT-BATAN.

6. References

[1] International Energy Agency (IEA), Key World Energy Statistics, in, 2017.

[2] Brandon Owens and John McGuinness, GE-Fuel Cells the Power of Tomorrow, General Electric Company, 2015.

[3] Abdalla M. Abdalla, Shahzad Hossain, Atia T. Azad, Pg Mohammad I. Petra, Feroza Begum, Sten G. Eriksson and Abul K. Azad, Nanomaterials for solid oxide fuel cells: A review, *Renewable and Sustainable Energy Reviews*, 82, (2018) 353-368 https://doi.org/10.1016/j.rser.2017.09.046

[4] Atiek Rostika Noviyanti, Ferli S. Irwansyah, Sahrul Hidayat, Arie Hardian, Dani Gustaman Syarif, Yati B. Yuliyati and Iwan Hastiawan, Preparation and conductivity of composite apatite $La_{9.33}Si_6O_{26}$ (LSO) - $Zr_{0.85}Y_{0.15}O_{1.925}$ (YSZ), *AIP Conference Proceedings*, 1712, 1, (2016) 050002 http://dx.doi.org/10.1063/1.4941885

[5] Qingle Shi, Hua Zhang, Tianjing Li, Fangli Yu, Haijun Hou and Pengde Han, Preparation and characterization of LSO-SDC composite electrolytes, *Journal of Rare Earths*, 33, 3, (2015) 304-309 https://doi.org/10.1016/S1002-0721(14)60418-X

[6] Mitsumasa Sakao, Tsuguo Ishihara and Hideki Yoshioka, Fabrication and ionic conductivity of oriented lanthanum silicate films with apatite-type structure, *Solid State Ionics*, 293, (2016) 51-55 https://doi.org/10.1016/j.ssi.2016.05.018

[7] Siddhartha Pathak, David Steinmetz, Jakob Kuebler, E. Andrew Payzant and Nina Orlovskaya, Mechanical behavior of $La_{0.8}Sr_{0.2}Ga_{0.8}Mg_{0.2}O_3$ perovskites, *Ceramics International*, 35, 3, (2009) 1235-1241 https://doi.org/10.1016/j.ceramint.2008.06.013

[8] Arup Mahata, Pradyot Datta and Rajendra N. Basu, Synthesis and characterization of Ca doped $LaMnO_3$ as potential anode material for solid oxide electrolysis cells, *Ceramics International*, 43, 1, Part A, (2017) 433-438 https://doi.org/10.1016/j.ceramint.2016.09.177

[9] D. Marrero-López, M. C. Martín-Sedeño, J. Peña-Martínez, J. C. Ruiz-Morales, P. Núñez, M. A. G. Aranda and J. R. Ramos-Barrado, Evaluation of apatite silicates as solid oxide fuel cell electrolytes, *Journal of Power Sources*, 195, 9, (2010) 2496-2506 https://doi.org/10.1016/j.jpowsour.2009.11.068

[10] V. Thangadurai and W. Weppner, Recent progress in solid oxide and lithium ion conducting electrolytes research, *Ionics*, 12, 1, (2006) 81-92 http://dx.doi.org/10.1007/s11581-006-0013-7

[11] Kiyoshi Kobayashi and Yoshio Sakka, Research progress in nondoped lanthanoid silicate oxyapatites as new oxygen-ion conductors, *Journal of the Ceramic Society of Japan*, 122, 1431, (2014) 921-939 http://dx.doi.org/10.2109/jcersj2.122.921

[12] S. Hui, X. Ma, H. Zhang, J. Dai, J. Roth, T. D. Xiao and D. E. Reisner, Plasma Sprayed LSGM Electrolyte for Intermediate Temperature Solid Oxide Fuel Cells, *ECS Proceedings Volumes*, 2003-07, (2003) 330-338 http://dx.doi.org/10.1149/200307.0330PV

[13] Morris Argyle and Calvin Bartholomew, Heterogeneous Catalyst Deactivation and Regeneration: A Review, *Catalysts*, 5, 1, (2015) 145 https://doi.org/10.3390/catal5010145

[14] Masahiro Kajitani, Motohide Matsuda, Akinori Hoshikawa, Ken-ichi Oikawa, Shuki Torii, Takashi Kamiyama, Fujio Izumi and Michihiro Miyake, Neutron Diffraction Study on Lanthanum Gallate Perovskite Compound Series, *Chemistry of Materials*, 15, 18, (2003) 3468-3473 http://dx.doi.org/10.1021/cm030294y

[15] Atiek Rostika Noviyanti, Bambang Prijamboedi, I Nyoman Marsih and Ismunandar Ismu, Hydrothermal Preparation of Apatite-Type Phases $La_{9.33}Si_6O_{26}$ and $La_9M_1Si_6O_{26.5}$ (M = Ca, Sr, Ba), *Journal of Mathematical and Fundamental Sciences*, 44, 2, (2013) 193-203 http://dx.doi.org/10.5614/itbj.sci.2012.44.2.8.

[16] Atiek Noviyanti, Juliandri, A. S. Utari and Yoga Trianzar Malik, Influence of synthesis time on lanthanum silicate apatite ($La_{9.33}Si_6O_{26}$) properties, *Research Journal of Chemistry and Environment*, 22, (2018) 120-123

[17] Natarajan Thenmozhi and Ramachandran Saravanan, High-temperature synthesis and electronic bonding analysis of Ca-doped LaMnO3 rare-earth manganites, *Rare Metals*, (2017) http://dx.doi.org/10.1007/s12598-017-0964-z

[18] Anindya Pal, Sudeep Paul, Amit Roy Choudhury, Vamsi Krishna Balla, Mitun Das and Arijit Sinha, Synthesis of hydroxyapatite from Lates calcarifer fish bone for biomedical applications, *Materials Letters*, 203, (2017) 89-92 https://doi.org/10.1016/j.matlet.2017.05.103

[19] Benoît Philippeau, Fabrice Mauvy, Cécile Mazataud, Sébastien Fourcade and Jean-Claude Grenier, Comparative study of electrochemical properties of mixed conducting $Ln_2NiO_{4+\delta}$ (Ln=La, Pr and Nd) and $La_{0.6}Sr_{0.4}Fe_{0.8}Co_{0.2}O_{3-\delta}$ as SOFC cathodes associated to $Ce_{0.9}Gd_{0.1}O_{2-\delta}$, $La_{0.8}Sr_{0.2}Ga_{0.8}Mg_{0.2}O_{3-\delta}$ and $La_9Sr_1Si_6O_{26.5}$ electrolytes, *Solid State Ionics*, 249-250, (2013) 17-25 https://doi.org/10.1016/j.ssi.2013.06.009

[20] Fitria Rahmawati, Bambang Prijamboedi, Syoni Soepriyanto and Ismunandar, SOFC composite electrolyte based on LSGM-8282 and zirconia or doped zirconia from zircon concentrate, *International Journal of Minerals, Metallurgy, and Materials*, 19, 9, (2012) 863-871 http://dx.doi.org/10.1007/s12613-012-0640-0

[21] K. Huang and J. B. Goodenough, Solid Oxide Fuel Cell Technology: Principles, Performance and Operations, Elsevier Science, 2009.

[22] Anna Magrasó, Marie-Laure Fontaine, Rune Bredesen, Reidar Haugsrud and Truls Norby, Cathode compatibility, operation, and stability of LaNbO4-based proton conducting fuel cells, *Solid State Ionics*, 262, (2014) 382-387 https://doi.org/10.1016/j.ssi.2013.12.009

[23] Deni S. Khaerudini, Guoqing Guan, Peng Zhang, Xiaogang Hao, Zhongde Wang, Chunfeng Xue, Yutaka Kasai and Abuliti Abudula, Performance assessment of $Bi_{0.3}Sr_{0.7}Co_{0.3}Fe_{0.7}O_{3-\delta}$-LSCF composite as cathode for intermediate-temperature solid oxide fuel cells with $La_{0.8}Sr_{0.2}Ga_{0.8}Mg_{0.2}O_{3-\delta}$ electrolyte, *Journal of Power Sources*, 298, (2015) 269-279 https://doi.org/10.1016/j.jpowsour.2015.08.075

[24] Xiao Guo Cao and San Ping Jiang, Identification of oxygen reduction processes at (La,Sr)MnO3

electrode/La9.5Si6O26.25 apatite electrolyte interface of solid oxide fuel cells, *International Journal of Hydrogen Energy*, 38, 5, (2013) 2421-2431 https://doi.org/10.1016/j.ijhydene.2012.12.043

[25] Y. Sakaki, Y. Takeda, A. Kato, N. Imanishi, O. Yamamoto, M. Hattori, M. Iio and Y. Esaki, Ln1-xSrxMnO3 (Ln=Pr, Nd, Sm and Gd) as the cathode material for solid oxide fuel cells, *Solid State Ionics*, 118, 3, (1999) 187-194 https://doi.org/10.1016/S0167-2738(98)00440-8